

## Author's Accepted Manuscript

The impact of fireworks on airborne particles

Roberta Vecchi, Vera Bernardoni, Diana Cricchio,  
Alessandra D' Alessandro, Paola Fermo, Franco Lucarelli,  
Silvia Nava, Andrea Piazzalunga, Gianluigi Valli

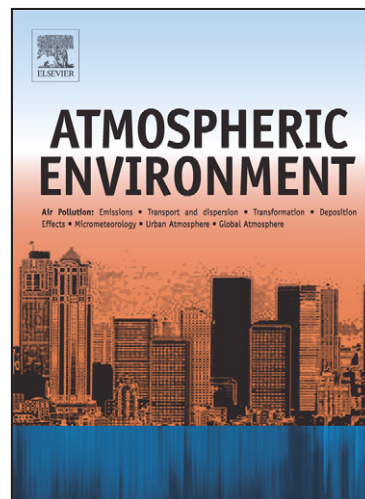
PII: S1352-2310(07)00968-5  
DOI: doi:10.1016/j.atmosenv.2007.10.047  
Reference: AEA 7897

To appear in: *Atmospheric Environment*

Received date: 7 June 2007  
Revised date: 22 October 2007  
Accepted date: 26 October 2007

Cite this article as: Roberta Vecchi, Vera Bernardoni, Diana Cricchio, Alessandra D' Alessandro, Paola Fermo, Franco Lucarelli, Silvia Nava, Andrea Piazzalunga and Gianluigi Valli, The impact of fireworks on airborne particles, *Atmospheric Environment* (2007), doi:10.1016/j.atmosenv.2007.10.047

This is a PDF file of an unedited manuscript that has been accepted for publication. As a service to our customers we are providing this early version of the manuscript. The manuscript will undergo copyediting, typesetting, and review of the resulting galley proof before it is published in its final citable form. Please note that during the production process errors may be discovered which could affect the content, and all legal disclaimers that apply to the journal pertain.



[www.elsevier.com/locate/atmosenv](http://www.elsevier.com/locate/atmosenv)

## The impact of fireworks on airborne particles

Roberta Vecchi<sup>\*1</sup>, Vera Bernardoni<sup>1</sup>, Diana Cricchio<sup>1</sup>, Alessandra D'Alessandro<sup>1</sup>, Paola Fermo<sup>2</sup>, Franco Lucarelli<sup>3</sup>, Silvia Nava<sup>4</sup>, Andrea Piazzalunga<sup>2</sup>, Gianluigi Valli<sup>1</sup>

<sup>1</sup>Inst. of Applied General Physics, University of Milan, and INFN-Milan, 20133, Milan, Italy

<sup>2</sup>Dep. of Inorganic, Metallorganic and Analytical Chemistry, University of Milan, 20133, Milan, Italy

<sup>3</sup>Dep. of Physics, University of Florence, and INFN-Florence, 50019, Florence, Italy

<sup>4</sup>National Inst. of Nuclear Physics, Sesto Fiorentino, 50019, Florence, Italy

### Abstract

Fireworks are one of the most unusual sources of pollution in atmosphere; although transient, these pollution episodes are responsible for high concentrations of particles (especially metals and organic compounds) and gases. In this paper, results of a study on chemical-physical properties of airborne particles (elements, ions, organic and elemental carbon and particles size distributions) collected during a fireworks episode in Milan (Italy) are reported. Elements typically emitted during pyrotechnic displays increased in one hour as follows: Sr (120 times), Mg (22), Ba (12), K (11), and Cu (6). In our case study, Sr was recognised as the best fireworks tracer because its concentration was very high during the event and lower than, or comparable with, minimum detection limits during other time intervals, suggesting that it was mainly due to pyrotechnic displays. In addition, particles number concentrations increased significantly during the episode (up to 6.7 times in one hour for the  $0.5 < d < 1 \mu\text{m}$  size bin). Contributions (e.g. Cu, elemental carbon and nitrogen oxides) to air pollution due to the large traffic volume registered during the same night were also singled out.

The original application of Positive Matrix Factorization and Multiple Linear Regression allowed, as far as we know, here for the first time, the quantification of the fireworks contribution to atmospheric particulate matter and the resolution of their chemical profile. The contribution of fireworks to the local environment in terms of PM10 mass, elements and chemical components was assessed with 4-hour time resolution. PM10 mass apportioned by fireworks was up to  $33.6 \mu\text{g m}^{-3}$  (about 50% of the total PM10 mass). Major contributors were elemental and organic carbon ( $2.8$  and  $8.1 \mu\text{g m}^{-3}$ , respectively) as well as metals like Mg, K, Sr, Ba, and Cu ( $0.4$ ,  $0.7$ ,  $0.07$ ,  $0.1$ , and  $0.1 \mu\text{g m}^{-3}$ , respectively).

*Keywords:* fireworks, chemical composition, number size distribution, PMF

---

\*Corresponding author: e-mail: [roberta.vecchi@unimi.it](mailto:roberta.vecchi@unimi.it) (R. Vecchi)

Tel +39 02 50317498 Fax +39 02 50317496

## 1. Introduction

In recent years concern for air pollution effects both on short-term and on long term has increased (Pope and Dockery, 2006; and therein literature). Therefore, many studies are currently carried out to characterise anthropogenic emissions especially in urban areas where large populations live.

One of the most unusual sources of pollution in atmosphere is the displacement of fireworks to celebrate festivities worldwide as well as specific events. The burning of fireworks is a huge source of gaseous pollutants such as ozone, sulphur dioxide, and nitrogen oxides (Attri et al., 2001; Ravindra et al., 2003) as well as of suspended particles. The aerosol particles emitted by fireworks are generally composed of metals (e.g. potassium, magnesium, strontium, barium, and copper), elemental carbon and secondary compounds like nitrate and organic substances (Kulshrestha et al., 2004; Drewnick et al., 2006; Moreno et al., 2007; Wang et al., 2007). The issue of exposure to elevated particle concentrations during celebrations with fireworks has implications in many countries of the world where pyrotechnic exhibitions often last for several hours/days (e.g. during Diwali Festival in India, Las Fallas in Spain, Lantern Festival in Beijing and New Year's celebration world-wide). The complex nature of particles emitted during fireworks may cause adverse health effects as reported in Ravindra et al. (2001). Nevertheless, some authors (Perry, 1999; Dutcher et al., 1999) concluded that fireworks unlikely pose a significant public health hazard, as they are relatively rare, detonate at altitudes well above the ground and generally burn outdoors, where the emitted pollutants can be dispersed in a large volume of air.

An additional effect of fireworks is the visibility reduction due to the generation of a dense cloud of smoke that drifts downwind and slowly disperses. The impact of fireworks on visibility and human health is particularly evident when the pyrotechnic exhibition is performed during stable meteorological conditions (Clark, 1997).

In this paper, we report on the chemical-physical characteristics of ambient aerosol measured during fireworks burnt in Milan (Italy) to celebrate the win of the football World Cup; due to the short duration of the fireworks exhibition, we considered it as a case study. The main goal of this paper is the assessment of the fireworks emissions environmental impact through the aerosol characterisation in terms of number (10 min resolution), mass and chemical composition (4-hour time resolution) as well as 1-hour resolution elemental data. In addition to particulate matter, trace gases concentrations, meteorological parameters, and atmospheric stability conditions were taken into account. Owing to the occurrence of this episode during a longer monitoring campaign, the apportionment of the fireworks source was possible applying Positive Matrix Factorization (PMF) and Multiple Linear Regression (MLR) to the whole dataset; as far as we know, this is the first attempt to identify and quantify the fireworks source contribution using a receptor model.

## 2. Experimental

The effect of pyrotechnic displays on air quality was studied in Milan (Italy) in July 2006, during the night between 9<sup>th</sup> and 10<sup>th</sup>, when the Italian team was celebrated for the win of the 2006 FIFA World Cup.

### 2.1 Site and sampling

Major pyrotechnic displays were located in the Cathedral's square downtown Milan; additional celebrations with many minor fireworks displays and a huge amount of crackers and sparkles were burnt everywhere in the town, starting soon after the end of the football match (at about 10:45 p.m.). Due to the peculiarity of the episode, the duration of the celebrations is not easy to assess (a reasonable estimate might be approximately 1 - 2 hours). The samplings were carried out at the University campus on the roof of the Institute of Physics, at about 10 m a.g.l.. The monitoring station was about 3 km far from the city centre so that the measurement related to the advected and diffused smoke cloud (as generally done in literature studies on this topic).

PM<sub>10</sub> was sampled starting at 12 a.m., local time, from July 9<sup>th</sup> to 11<sup>th</sup>, every 4 hours. Samplings were carried out in parallel on PTFE filters (diameter: 47 mm, pore size: 2  $\mu\text{m}$ ) and quartz fibre filters (diameter: 47 mm, pre-fired at 700°C for 1 hour) using CEN-equivalent samplers operating at a flow rate of 2.3 m<sup>3</sup> h<sup>-1</sup>.

Fine ( $d_{ac} < 2.5 \mu\text{m}$ ) and coarse ( $2.5 < d_{ac} < 10 \mu\text{m}$ ) PM fractions were also collected with hourly resolution, using a streaker sampler. The streaker sampler separates particles in two different stages using a pre-impactor (which removes particles with  $d_{ac} > 10 \mu\text{m}$ ) and an impactor. The latter is made of a Kapton foil on which coarse particles are collected. The fine fraction is then sampled on a Nuclepore filter (0.4  $\mu\text{m}$  pore diameter). The Kapton foil and Nuclepore filter are paired in a cartridge rotating at constant angular speed (1.8° h<sup>-1</sup>); this produces a circular continuous deposition on both stages. It should be noted that mass concentration in streaker samples is not available. Further details on the sampler, its cut-off diameters, and its control unit can be found elsewhere (Prati et al. 1998); it should be noticed that mass concentration in streaker samples is not available.

### 2.2 Laboratory analyses

Before and after the samplings the filters were exposed for 48 hours on open but dust-protected sieve-trays in an air-conditioned weighing room ( $T = 20 \pm 1 \text{ }^\circ\text{C}$  and R.H. = 50  $\pm$  5 %). The gravimetric determination of the mass was carried out using an analytical microbalance (precision 1  $\sigma\text{g}$ ), which was installed and operated in the weighing room. Calibration procedures checked the microbalance performance.

PTFE filters were analysed for elemental composition by Energy Dispersive X-Ray Fluorescence technique (details can be found in Marcazzan et al., 2004), obtaining concentration values for Mg, Al, Si, S, Cl, K, Ca, Ti, Cr, Mn, Fe, Ni, Cu, Zn, Br, Sr, Ba, Pb. Other elements (i.e. V, As, Se, Zr, and Mo) were in principle detectable, but they often resulted below the minimum detection limit (MDL), which was in the range 2 – 20 ng m<sup>-3</sup> for most elements. Experimental overall uncertainties were in the range 10-15 %.

One half of the quartz fibre filters was analysed for water-soluble major components ( $\text{SO}_4^{2-}$ ,  $\text{NO}_3^-$ , and  $\text{NH}_4^+$ ) by ion chromatography (IC). A special care was used in IC analyses of particulate matter collected on quartz fibre filters due to

high blank levels (minimum detection limits: 167, 359 e 46 ng m<sup>-3</sup> for SO<sub>4</sub><sup>2-</sup>, NO<sub>3</sub><sup>-</sup>, and NH<sub>4</sub><sup>+</sup>, respectively); information about extraction procedures and blanks correction can be found in Fermo et al. (2006). The overall uncertainty for ionic concentrations was estimated in 10 %.

One punch (area: 1.5 cm<sup>2</sup>) cut from the quartz fibre filter was analysed by TOT (Thermal-Optical Transmittance) method (Birch and Cary, 1996) to quantify elemental and organic carbon. The technique detection limit was 0.2 σgC m<sup>-3</sup> and the precision was 5%.

Nuclepore and Kapton substrates from the streaker sampler were analysed by Particle Induced X-ray Emission analysis (PIXE) at the LABEC-INFN accelerator facility in Florence, Italy, whose set up is described in Calzolari et al. (2006). The concentration of 19 elements (Na, Mg, Al, Si, S, Cl, K, Ca, Ti, Cr, Mn, Fe, Ni, Cu, Zn, Br, Sr, Ba, Pb) was obtained. As for ED-XRF analysis, other elements were in principle detectable, but they often were below the minimum detection limit (lower than 10 ng m<sup>-3</sup> for V, As, Se, Zr, Rb, Mo). The accuracy of hourly elemental concentrations was in the range 2% - 20%.

### 2.3 Additional measurements

An Optical Particle Counter (Grimm, mod.1.107) measured number size distributions in the 0.25-32 σm range (31 size bins).

To evaluate atmospheric dispersion conditions, <sup>222</sup>Rn short-lived decay products measurements were performed using the experimental methodology reported in Marcazzan et al. (2003). Mixing layer heights (MLH) with hourly resolution were obtained by means of a box model suitably set up by the group of the Institute of Physics using <sup>222</sup>Rn concentration measurements as input data (Pacifico, 2005). MLH evaluations by our box-model were in good agreement with thermal inversions heights from radio-soundings data by the nearby Milan-Linate airport as well as with other modelling studies based on thermodynamic variables (Casadei et al., 2006).

Meteorological parameters (wind speed and direction, relative humidity, pressure, temperature, solar radiation and precipitation) were also measured at the Institute of Physics monitoring station.

Trace gases data recorded at monitoring stations of the Regional Environmental Protection Agency were also available (Figure 1): NO<sub>2</sub> and NO at the 1-J station (near the University campus and the motor-way) and NO<sub>2</sub>, NO and CO at the 2-V station (city centre) and 3-L (on the ring-round). Moreover, hourly traffic volumes in the city centre were recorded at the station 4-S (city centre).

### 2.4 Receptor model

The fireworks episode occurred during a longer field campaign, which was performed during two weeks in summer and two weeks in winter 2006, with the same characteristics as those described in paragraphs 2.1, 2.2, and 2.3. The complete

PM10 data set (180 samples) was analysed by PMF to identify and apportion (by MLR) major aerosol sources. PMF resolved seven sources (re-suspended soil, construction works, industry, traffic, secondary sulphates, secondary nitrates and fireworks). In this paper, only results on the fireworks source will be described and discussed (another paper in preparation deals with the other six sources).

PMF is an advanced factor analysis technique computing a weighted, non-negative constrained least squares fit. It imposes non-negativity constraints to the factors and uses realistic error estimates from data standard deviations, as described in Paatero (1997). Data values and errors, missing values and below detection limit data were calculated according to Polissar et al. (1998) and used in this work as inputs for the PMF.

In PMF studies, a weak variable (according to signal to noise ratio criterion, as in Paatero and Hopke, 2003) can sometimes be inserted in the fit with the normal variables if it represents a tracer of a specific source (Qin et al., 2006). This approach was here adopted for Sr, considered the best tracer of the fireworks source in our case study (see paragraph 3.3). It was not really a weak variable but it had a much lower signal to noise ratio respect to other variables. In this work, instead of reducing the weights of Sr, we doubled them to highlight the role of this fireworks tracer in the fit. At the same time, it was necessary to down-weight some variables by increasing their uncertainties by a factor from 2 to 4 to obtain a better distribution of their scaled residuals (Kim et al., 2003). The coefficients of adjustment for the weights were determined with trial and error method until the model resolved the fireworks source, together with the same six sources found in a previous analysis where Sr was not used as input for PMF.

Rotational ambiguity is always a problem in factor analysis (Paatero et al., 2002); in this work, after a systematic study of the rotational range of the solution, FPEAK=0 was chosen. MLR was performed to regress the total mass against the factor scores; the regression coefficients were then used to transform the factor profiles given in arbitrary units in parts per million ones and to quantitatively apportion the mass contributions among the resolved sources.

### 3. Results and discussion

#### 3.1 Mass concentration and meteorological conditions

During the case study period, meteorological conditions were quite stable. The wind speed was about  $1 \text{ m s}^{-1}$  as average value between 10:30 p.m. and 12 a.m. on the fireworks night and the prevalent wind direction was changing from south-westerly to westerly direction.

During the fireworks night a  $^{222}\text{Rn}$  strong accumulation was registered (Figure 2); the variation of Radon concentration between the minimum ( $8.6 \text{ Bq m}^{-3}$ ) on July 9<sup>th</sup> afternoon and the maximum ( $26.4 \text{ Bq m}^{-3}$ ) in the following day was a good indicator of the nocturnal mixing layer depth, which was lower than 100 m.

In Figure 2, PM10 mass and  $^{222}\text{Rn}$  concentration on 9<sup>th</sup>-10<sup>th</sup> July 2006 are shown. On 10<sup>th</sup> July, PM10 concentration increased up to  $63.9 \text{ } \mu\text{g m}^{-3}$  in the time interval between 12 a.m. and 4 a.m., when the pyrotechnical displays contribution

was maximum at our monitoring station, as singled out by the chemical markers analysis (see paragraph 3.3). However, fireworks were not likely the only cause of PM<sub>10</sub> growth during that night; indeed, the concomitant strong accumulation of <sup>222</sup>Rn concentration suggests that this increase was likely due both to sources emissions and to the strong atmospheric stability.

As far as we know, currently in the literature there is no quantification of the fireworks contribution to the PM mass, as this estimation is difficult and not straightforward. With the aim of apportioning the fireworks source, in this paper the receptor model approach has been possible owing to the availability of a large number of chemically characterised PM samples with 4-hours temporal resolution. According to the PMF source apportionment the fireworks contribution began to be remarkable in the 8 p.m. – 12 a.m. time interval, accounting for 13.1  $\mu\text{g m}^{-3}$  of the PM<sub>10</sub> mass (27 %), reached its maximum at 33.6  $\mu\text{g m}^{-3}$  (53 %) in the 4 hours after midnight and decreased to 4.2  $\mu\text{g m}^{-3}$  (8 %) from 4 a.m. to 8 a.m.

### 3.2 Gaseous pollutants

CO concentration and traffic volumes increased soon after the end of the match (10:45 p.m.) at the monitoring stations 2-V and 4-S near the Cathedral's Square, as shown in Figure 3a. A similar pattern in CO concentration, i.e. maximum value between 11 p.m. and 12 a.m. with a 3-fold increase in one hour, was also recorded at the station 3-L, located next to the city ring-road (see Figure 1) and about 1.5 km far from major pyrotechnic displays. In Figure 3b NO<sub>2</sub> temporal patterns recorded at the stations 2-V, 3-L and 1-J are reported. At the 2-V and 3-L stations the concentration increase was recorded simultaneously with the CO increase while at the station 1-J (near University Campus) a delay in the maximum concentration occurred.

Ravindra et al. (2003) observed NO<sub>2</sub> increases during the pyrotechnic displays. On the contrary, in our case the experimental results indicate that the increase in trace gases concentration was mainly due to the high number of vehicles circulating soon after the end of the match to celebrate the national team more than to fireworks emissions. Indeed, it is important to observe that the location of the 3-L monitoring station compared to the city centre and the prevalent wind direction (see paragraph 3.1) suggest that fireworks unlikely affect air quality in that area. Moreover, the NO<sub>2</sub> temporal trend observed at the station near major pyrotechnic displays (2-V) and at the 3-L station are comparable, indicating that no significant NO<sub>2</sub> emissions can be ascribed to fireworks in our case study. The NO<sub>2</sub> peak occurring at 2 a.m. in the 1-J station was explained by traffic flows, likely due to people going back home, as also confirmed by Cu temporal pattern (another traffic tracer) represented in Figure 4.

### 3.3 Chemical composition

On 9<sup>th</sup> July, starting from 11 p.m., the hourly concentrations of some elements in the fine fraction strongly increased. Similar results were also found PM<sub>10</sub> elemental data with 4-hour resolution (in Table 1 mass and chemical components

concentrations are given for the episode); nevertheless, for sake of brevity, the data with the highest time resolution are represented in Figure 4. At our monitoring station, the highest values were registered on 10<sup>th</sup> July between 1 a.m. and 2 a.m.; this is consistent with the location of major fireworks considering wind speed and direction. To quantify the elements concentration increase during the episode, the maximum concentration was compared to the value of the day before (9<sup>th</sup> July, not affected by fireworks), averaged between 12 a.m. and 10 p.m. In case of below MDL hourly data, one-half of the MDL value was used. Remarkable increases in Sr (120 times), Mg (22 times), K (12 times), Ba (11 times), and Cu (6 times) concentration were observed. No increases were detected in the coarse fraction elemental concentrations and Sr, Mg, K, Ba, and Cu concentrations were below or comparable to MDL (not shown), indicating that ambient aerosol after the fireworks event was preferably confined in the fine fraction.

Sr, Ba, and Cu compounds are used to give red, green, and blue fireworks, respectively (Kulshrestha et al., 2004; Wang et al., 2007; Moreno et al., 2007). Different Ba compounds can give the green colour, but the increase in chlorine concentration measured during the fireworks night and the nitrate concentration comparable or lower than other nights one, suggested that Ba(ClO<sub>3</sub>)<sub>2</sub> was more likely used (Perry, 1999). K is one of the major components of fireworks (Liu et al., 1997; Dutcher et al., 1999; Perry, 1999; Kulshrestha et al., 2004; Drewnick et al., 2006): 74% of black powder consists of KNO<sub>3</sub>, which provides the main oxidizer to the burning. Also potassium perchlorate or, less commonly, chlorate can be used in the black powder. Mg gives origin to bright electric white fireworks and it is used as metallic fuel (Moreno et al., 2007; Wang et al. 2007).

In this work, Sr was recognised as the best fireworks tracer because its concentration was very high during the event and lower than, or comparable with, MDL during other time intervals, suggesting that it was mainly due to pyrotechnic displays (see also PMF results in Table 2). On the contrary, Cu and Ba can also have a contribution coming from traffic (Vecchi et al., 2007 and therein literature) and K and Mg are widespread elements emitted by many sources (e.g. biomass burning for K and soil dust for Mg).

From 4-hours resolution PM<sub>10</sub> data, the concentration ratios between levels registered in the 12 a.m. - 4 a.m. time interval and the average values of the day before (during the period free from the event, i.e. between 12 a.m. and 8 p.m.) were calculated; results for elements, organic and elemental carbon, and ions are reported in Figure 5. As expected, the most significant increases were observed for Sr, Mg, Ba, K, and Cu (elements ratios were smaller than those reported for 1-hour resolution elemental data because the longer sampling time included periods with lower concentrations). Indeed, these elements can be all considered fireworks tracers.

The nitrate concentration ratio was comparable to the one measured during other summer nights at the same sampling site (as an example, see the comparison with 6<sup>th</sup> July night, in Figure 5) because of the lower night-time temperature, which limited losses due to volatilisation. In agreement with results by Drewnick et al. (2006), in our case study no nitrate increase due to fireworks was observed.



The EC ratios (3.1) found in this work are in good agreement with black carbon increases reported by Babu and Moorthy (2001) and by Wang et al. (2007).

Opposite to what found by Wang et al (2007), no anomalous growth in secondary components was observed the day after the pyrotechnical displacement: the increases in sulphate and ammonium were similar to the ones measured during other summer afternoons at the same sampling site. However, it should be taken into account that secondary compounds formation may change in relation to local meteorological condition, pollutants mixture and duration and strength of the episode.

In Figure 6, the fireworks chemical profile obtained by PMF is also reported as an original contribution to the characterisation of fireworks emissions. Major components are carbon compounds (both EC and OC) and metals. The fireworks source profile confirms Sr as the best tracer in our case study as, contrarily to other fireworks indicators, it was found only in this chemical profile while, for example, Ba was also detected in the traffic profile, and K was found in a number of sources (not shown here). In Table 2 the PMF apportionment for major PM10 components detected during pyrotechnic displays is reported. As already reported for PM10 mass concentrations, also elements, ions, and carbon components peaked in the 12 a.m. - 4 a.m. time interval. Total carbon (TC = EC+OC) due to fireworks accounted for  $11 \mu\text{g m}^{-3}$  of the PM10 mass (i.e. about 50-55 % of the measured total carbon). Major elemental contributions apportioned by PMF and due to the pyrotechnic displays were Mg ( $0.4 \mu\text{g m}^{-3}$ ), K ( $0.7 \mu\text{g m}^{-3}$ ), Cu ( $0.07 \mu\text{g m}^{-3}$ ), Sr ( $0.1 \mu\text{g m}^{-3}$ ), and Ba ( $0.1 \mu\text{g m}^{-3}$ ) corresponding to 81%, 77%, 68%, 100% and 91% of their measured concentration, respectively. These results are in very good agreement with experimental observations discussed so far.

### 3.4 Number size distribution

During the fireworks night, starting from 11 p.m., the number concentration in all size ranges increased. The growths were different for each size bin, but the maximum concentration was always found on 12:10 a.m.. The ratios between the number of particles measured on 12:10 a.m. and 11 p.m. were as follows: 6.7 for particles in the range  $0.5 < d < 1 \mu\text{m}$ , 2.8 for particles in the range  $2.5 < d < 10 \mu\text{m}$ , 2.6 for particles in the range  $1 < d < 2.5 \mu\text{m}$  and 1.7 for particles with  $d < 0.5 \mu\text{m}$ . The delay (about 1.5 hours) in the occurrence of the maximum concentration compared to end of the match may be explained considering the distance of our sampling site from the city centre (where the major fireworks exhibition was performed and the largest traffic volume observed) together with the low wind speed, the wind direction and the atmospheric stability conditions. From 12:10 a.m. to 1:40 a.m. the particles number concentration in all size ranges decreased as follows: -20% for particles with  $d < 0.5 \mu\text{m}$ , -70% for particles in the range  $0.5 < d < 1 \mu\text{m}$ , -50% for particles in the  $1 < d < 2.5 \mu\text{m}$  range and -35% for particles in  $2.5 < d < 10 \mu\text{m}$  range. Between 1:40 a.m. and 3 a.m. another increase was observed in all size bins, and particularly in particles with diameters smaller than  $0.4 \mu\text{m}$ . It is interesting to note that a growth in Cu hourly concentration (fine fraction) and in  $\text{NO}_2$  concentration (at 1-J monitoring station near the University

campus) was also measured between 2 a.m. and 3 a.m. (see Figures 3b and 4). As these increases were contemporary, the growth in particle number concentration might be ascribed to traffic (contributing to Cu, NO<sub>2</sub>, and fine particles), because of people going back home after celebrations. Moreover, these results suggested that traffic emissions were mainly in the finest fractions. After 3 a.m., particles number concentrations definitively decreased until the next morning, when the number of particles increased again because of typical working day's activities.

Particles number temporal pattern in each size range was compared to Sr concentration (taken here as fireworks tracer). The correlation coefficients between Sr (fine fraction) and number concentration were calculated using hourly-resolved data between 10 p.m. on 9<sup>th</sup> July and 10 a.m. on 10<sup>th</sup> July. The highest correlation coefficients ( $R > 0.95$ ) were registered in the 0.45 – 1  $\mu\text{m}$ , and particularly in the 0.70 - 0.80  $\mu\text{m}$ , size bin ( $R = 0.98$ ). The high correlation between Sr and the 0.7-0.8  $\mu\text{m}$  size range is consistent with what found by Perry (1999), who reported 0.7  $\mu\text{m}$  as mass mean diameter of potassium (in that work considered the indicator for fireworks) observed after fireworks emissions transport.

In Figure 7, Sr temporal pattern (1-hour resolution) and particles number concentrations (10-minutes resolution) in the 0.25-0.3  $\mu\text{m}$ , 0.70 - 0.80  $\mu\text{m}$ , and 8.5-10  $\mu\text{m}$  size intervals are shown, as examples. A very good agreement between Sr and particle number in the 0.70 - 0.80  $\mu\text{m}$  size range in the increase phase and in the first part of the decrease phase was evident, while differences can be noticed after 2 a.m. However, it must be considered that, in this case study, fireworks display was the only source of Sr while airborne particles in general can be originated by different sources. In Figure 7 can also be noted that, even if particles in the 0.25-0.3  $\mu\text{m}$  and 8.5-10  $\mu\text{m}$  size ranges increased during the fireworks period, a poorer correlation ( $R = 0.72$  and  $R = -0.13$ , respectively) was found with Sr concentration.

Taking into account the good correlation between Sr and particles in 0.4-1  $\mu\text{m}$  size range during the increase phase, and evaluating the time necessary to Sr to reach values similar to those presented before fireworks, a rough estimate of the time necessary to particles in this size-range to diffuse (with low wind speed conditions) can be evaluated in about 12 hours.

#### 4. Conclusions

The fireworks exhibition was used to study the chemical composition and the size distribution of airborne particles observed during such events. The influence of additional emissions due to the traffic registered just after the football match was also discussed.

Atmospheric aerosols originated by fireworks had a typical signature as singled out by the few works on this topic (see references given in the text). Results obtained by hourly elemental analysis showed that in the fine fraction many metals (i.e. Sr, Mg, K, Ba and Cu) increased significantly during the celebrations (e.g. Sr up to 120 times in one hour) while no differences were observed in the coarse fraction concentrations. It is worth noting that, although fireworks cause short-lived air pollution events, fine particles are responsible for adverse health effects, and the bioreactivity of fine metal aerosols is of particular concern (Moreno et al, 2007; and therein cited literature).

The availability of a large number of chemically characterised samples allowed the PM10 and major chemical components apportionment during the pyrotechnic displays. Although our fireworks event had short duration, the PM10 concentration ascribed by PMF to the fireworks source was not negligible (up to  $33.6 \mu\text{g m}^{-3}$ ). In addition, fireworks accounted for a large part of the metal concentrations (e.g. up to 70-100% of the measured values for Mg, K, Cu, Sr, and Ba). Obviously, the impact of this source type can vary considerably in relation to fireworks duration and type, being more serious when stable atmospheric conditions occur (Clark, 1997). The assessment of the fireworks source chemical profile and of the contribution of fireworks to local environment gives an original contribution towards understanding the aerosol characteristics and burden during fireworks displays.

#### Acknowledgements

The authors acknowledge ARPA Lombardia for providing data from the air quality monitoring network.

#### References

- €# Attri, A.K., Kumar, U., Jain, V.K., 2001. Formation of ozone by fireworks. *Nature* 411, 1015
- €# Babu, S.S., Moorthy, K.K., 2001. Anthropogenic impact on aerosol black carbon mass concentration at a tropical coastal station: a case study. *Current Science* 81, 1208-1214
- €# Birch, M.E., Cary, R.A., 1996. Elemental Carbon-based method for monitoring occupational exposures to particulate diesel exhaust. *Aerosol Science and Technology* 25, 221-241
- €# Calzolari, G., Chiari, M., García Orellana, I., Lucarelli, F., Migliori, A., Nava, S., Taccetti, F., 2006. The new external beam facility for environmental studies at the Tandatron accelerator of LABEC. *Nuclear Instruments and Methods in Physics Research B* 249, 1-2, 928-931

- €# Casadei, S., Giugliano, M., Lonati, G., Pacifico, F., Valli, G., Vecchi, R., 2006. Valutazione dell'altezza dello strato rimescolato nell'area urbana di Milano nel biennio 2003-2004. *Ingegneria Ambientale*, XXXV, 4, 155-168 (in Italian)
- €# Clark, H., 1997. Light blue touch paper and retire... *Atmospheric Environment* 31, 2893-2895
- €# Drewnick, F., Hings, S.S., Cutius, J., Eerdekens, G., Williams, J., 2006. Measurement of fine particulate matter and gas-phase species during the New Year's fireworks 2005 in Mainz, Germany. *Atmospheric Environment* 40, 4316-4327
- €# Dutcher, D.D., Perry, K.D., Cahill, T.A., Copeland, S.A., 1999. Effects of indoor pyrotechnic displays on the air quality in the Houston Astrodome. *Journal of Air & Waste Management Association* 49, 156-160
- €# Fermo, P., Piazzalunga, A., Vecchi, R., Valli, G., 2006. Set-up of extraction procedures for ions quantification in aerosol samples. *Chemical Engineering Transactions* 10, 203-208
- €# Kim, E., Larson, T.V., Hopke, P.K., Slaughter, C., Sheppard, L.E., Claiborn, C., 2003. Source identification of PM<sub>2.5</sub> in an arid Northwest U.S. City by positive matrix factorization. *Atmospheric Research* 66, 291-305
- €# Kulshrestha, U.C., Rao Nageswara, T., Azhaguvel, S., Kulshrestha, M.J., 2004. Emissions and accumulation of metals in the atmosphere due to crackers and sparkles during Diwali festival in India. *Atmospheric Environment* 38, 4421-4425
- €# Liu, D.Y., Rutherford, D., Kinsey, M., Prather, K.A., 1997. Real-Time Monitoring of Pyrotechnically Derived Aerosol Particles in the Troposphere. *Analytical Chemistry* 69, 1808-1814
- €# Marcazzan, G.M., Caprioli, E., Valli, G., Vecchi, R., 2003. Temporal variation of <sup>212</sup>Pb concentration in outdoor air of Milan and a comparison with <sup>214</sup>Bi. *Journal of Environmental Radioactivity*, 65, 77-90
- €# Marcazzan, G.M., Ceriani, M., Valli, G., Vecchi, R., 2004. Composition, components and sources of fine aerosol fractions using multielemental EDXRF analysis. *X-Ray Spectrometry* 33, 267-272
- €# Moreno, T., Querol, X., Alastuey, A., Minguillón, M.C., Pey, J., Rodriguez, S., Miró, J.V., Felis, C., Gibbons, W., 2007. Recreational atmospheric pollution episodes: inhalable metalliferous particles from fireworks displays. *Atmospheric Environment* 41, 913-922
- €# Paatero, P., 1997. Least squares formulation of robust non-negative factor analysis. *Chemometrics and Intelligent Laboratory Systems* 37, 23-35
- €# Paatero, P., Hopke, P.K., Song, X., Ramadan, Z., 2002. Understanding and controlling rotations in factor analytical models. *Chemometrics and Intelligent Laboratory Systems* 60, 253-264
- €# Paatero, P., Hopke, P.K., 2003. Discarding or downweighting high-noise variables in factor analytic models. *Analytica Chimica Acta* 490, 277-289
- €# Pacifico, F., 2005. Il Radon come tracciante dell'altezza dello strato rimescolato: sviluppo di un modello a box. Degree Thesis in Physics, University of Milan, Italy (in Italian)
- €# Perry, K.D., 1999. Effects of outdoor pyrotechnic displays on the regional air quality of Western Washington State. *Journal of Air & Waste Management Association* 49, 146-155

- €# Polissar, A.V., Hopke, P.K., Paatero, P., Malm, W.C., Sisler, J.F., 1998. Atmospheric aerosol over Alaska. 2. Elemental composition and sources. *Journal of Geophysical Research* 103, 19045-19057
- €# Pope Arden III, C., Dockery, D.W., 2006. Health effects of fine particulate air pollution: lines that connect. *Journal of Air and Waste Management Association* 56, 709-742
- €# Prati, P., Zucchiatti, A., Tonus, S., Lucarelli, F., Mandò, P.A., Ariola, V., 1998. A testing technique of streaker aerosol samplers via PIXE analysis. *Nuclear Instruments and Methods in Physics Research B* 136-138, 986-989
- €# Qin, Y., Kim, E., Hopke, P.K., 2006. The concentrations and sources of PM<sub>2.5</sub> in metropolitan New York City. *Atmospheric Environment* 40, S312-S332
- €# Ravindra, K., Mittal, A.K., Van Grieken, R., 2001. Health risk assessment of urban suspended particulate matter with special reference to polycyclic aromatic hydrocarbons: a review. *Reviews on Environmental Health* 16, 3, 169-189
- €# Ravindra, K., Mor, S., Kaushik, C.P., 2003. Short-term variation in air quality associated with fireworks events: a case study. *Journal of Environmental Monitoring* 5, 260-264
- €# Vecchi, R., Marcazzan, G., Valli, G., 2007. A study on nighttime-daytime PM<sub>10</sub> concentration and elemental composition in relation to atmospheric dispersion in the urban area of Milan (Italy). *Atmospheric Environment* 41, 2136-2144
- €# Wang, Y., Zhuang, G., Xu, C., An, Z., 2007. The air pollution caused by the burning of fireworks during the lantern festival in Beijing. *Atmospheric Environment* 41, 417-431

**Figure captions**

Figure 1: map of the monitoring stations.

Figure 2: PM10 mass (in  $\sigma\text{g m}^{-3}$ ) and  $^{222}\text{Rn}$  concentration (in  $\text{Bq m}^{-3}$ ) on 9<sup>th</sup>-10<sup>th</sup> July 2006 in Milan.

Figure 3: a) CO (in  $\text{mg m}^{-3}$ ) and traffic volume (number of vehicles); b) NO<sub>2</sub> (in  $\sigma\text{g m}^{-3}$ ) concentrations at three different monitoring stations on 9<sup>th</sup>-10<sup>th</sup> July 2006 in Milan.

Figure 4: fireworks elemental markers, fine fraction data with hourly resolution (in  $\text{ng m}^{-3}$ )

Figure 5: Ratios between the concentration of different chemical components registered in the time interval 12 a.m. - 4 a.m. (fireworks displays) on 9<sup>th</sup>-10<sup>th</sup> July night and the average value measured for the same species during the day before (grey). Similar ratios (white) calculated for the night between 6<sup>th</sup> and 7<sup>th</sup> July (free from fireworks) are given for comparison.

Figure 6: fireworks source profile (in  $\text{mg mg}^{-1}$ ) as resolved by PMF

Figure 7: Sr hourly temporal pattern (in  $\text{ng m}^{-3}$ ) together with particles number concentration (particles  $\text{m}^{-3}$ ) in the 0.25-0.30  $\sigma\text{m}$ , 0.70-0.80  $\sigma\text{m}$  and 8.5-10  $\sigma\text{m}$  size intervals

**Table captions**

Table 1: 4-hour resolution chemical components and elemental concentrations (in  $\text{ng m}^{-3}$ ) during the fireworks episode

Table 2: Contribution to PM10 mass and major chemical components concentration (in  $\text{ng m}^{-3}$  and as percentage of their measured concentration) due to the fireworks source obtained by PMF. By convention, concentration values lower than experimental minimum detection limits have been labelled as <MDL.

Table 1

Date	9/7	9/7	10/7	10/7	10/7	10/7
Time interval	4 p.m. - 8 p.m.	8 p.m. - 12 a.m.	12 a.m. - 4 a.m.	4 a.m. - 8 a.m.	8 a.m. - 12 p.m.	12 p.m. - 4 p.m.
PM10 mass	46 400	48 200	63 900	51 400	71 100	55 500
SO <sub>4</sub> <sup>2-</sup>	4 232	3 130	3 622	2 687	2 830	5 147
NO <sub>3</sub> <sup>-</sup>	<360	1 115	4 499	2 326	2 326	3 683
NH <sub>4</sub> <sup>+</sup>	1 169	1 102	1 575	868	1 644	2 548
OC	7 870	9 806	13 491	11 672	12 071	10 490
EC	1 293	1 959	5 372	4 070	4 694	1 748
Mg	<100	183	598	246	127	182
Al	355	519	680	451	720	609
Si	802	1 023	1 368	967	1 790	1 344
S	1 303	803	1 176	1 276	1 024	1 759
Cl	<70	<70	233	98	115	121
K	158	369	991	369	364	267
Ca	308	369	645	723	1 475	744
Ti	28	32	46	37	53	34
V	<6	<6	<6	<6	<6	<6
Cr	<4	<4	11	10	<4	<4
Mn	7	16	30	35	30	20
Fe	468	847	1 731	1 581	1 374	586
Ni	4	2	5	7	6	5
Cu	20	43	105	56	65	25
Zn	82	85	190	270	276	90
Br	5	6	9	12	6	4
Pb	9	16	57	25	41	14
Sr	<3	55	139	18	11	<3
Ba	<20	41	156	22	31	24

Table 2

		9/7	9/7	10/7	10/7	10/7	10/7
		4 p.m. - 8 p.m.	8 p.m. - 12 a.m.	12 a.m. - 4 a.m.	4 a.m. - 8 a.m.	8 a.m. - 12 p.m.	12 p.m. - 4 p.m.
<b>EC</b>	$ng\ m^{-3}$ (%)	<MDL	1 101 (56)	2 827 (54)	357 (9)	211 (6)	<MDL
<b>OC</b>	$ng\ m^{-3}$ (%)	<MDL	3 144 (39)	8 075 (52)	1 019 (9)	601 (5)	<MDL
<b>Mg</b>	$ng\ m^{-3}$ (%)	<MDL	168 (62)	433 (81)	<MDL	<MDL	<MDL
<b>Al</b>	$ng\ m^{-3}$ (%)	<MDL	102 (20)	262 (38)	<MDL	<MDL	<MDL
<b>Si</b>	$ng\ m^{-3}$ (%)	<MDL	151 (15)	387 (29)	49 (5)	29 (2)	<MDL
<b>K</b>	$ng\ m^{-3}$ (%)	<MDL	269 (64)	692 (77)	87 (27)	52 (13)	<MDL
<b>Ca</b>	$ng\ m^{-3}$ (%)	<MDL	111 (30)	284 (44)	36 (5)	21 (1)	<MDL
<b>Mn</b>	$ng\ m^{-3}$ (%)	<MDL	5.2 (33)	13 (44)	<MDL	<MDL	<MDL
<b>Fe</b>	$ng\ m^{-3}$ (%)	10.3 (2)	400 (48)	1 028 (57)	130 (10)	77 (5)	10 (1)
<b>Cu</b>	$ng\ m^{-3}$ (%)	<MDL	27 (66)	70 (68)	9 (14)	5 (9)	<MDL
<b>Zn</b>	$ng\ m^{-3}$ (%)	<MDL	38 (45)	98 (52)	12 (5)	7 (3)	<MDL
<b>Sr</b>	$ng\ m^{-3}$ (%)	<MDL	54 (100)	140 (100)	18 (99)	10 (98)	<MDL
<b>Ba</b>	$ng\ m^{-3}$ (%)	<MDL	51 (90)	130 (91)	16 (47)	<MDL	<MDL
<b>PM10 mass</b>	$ng\ m^{-3}$ (%)	<MDL	13 087 (27)	33 610 (53)	4 240 (8)	<MDL	<MDL



Figure 1



Figure 2

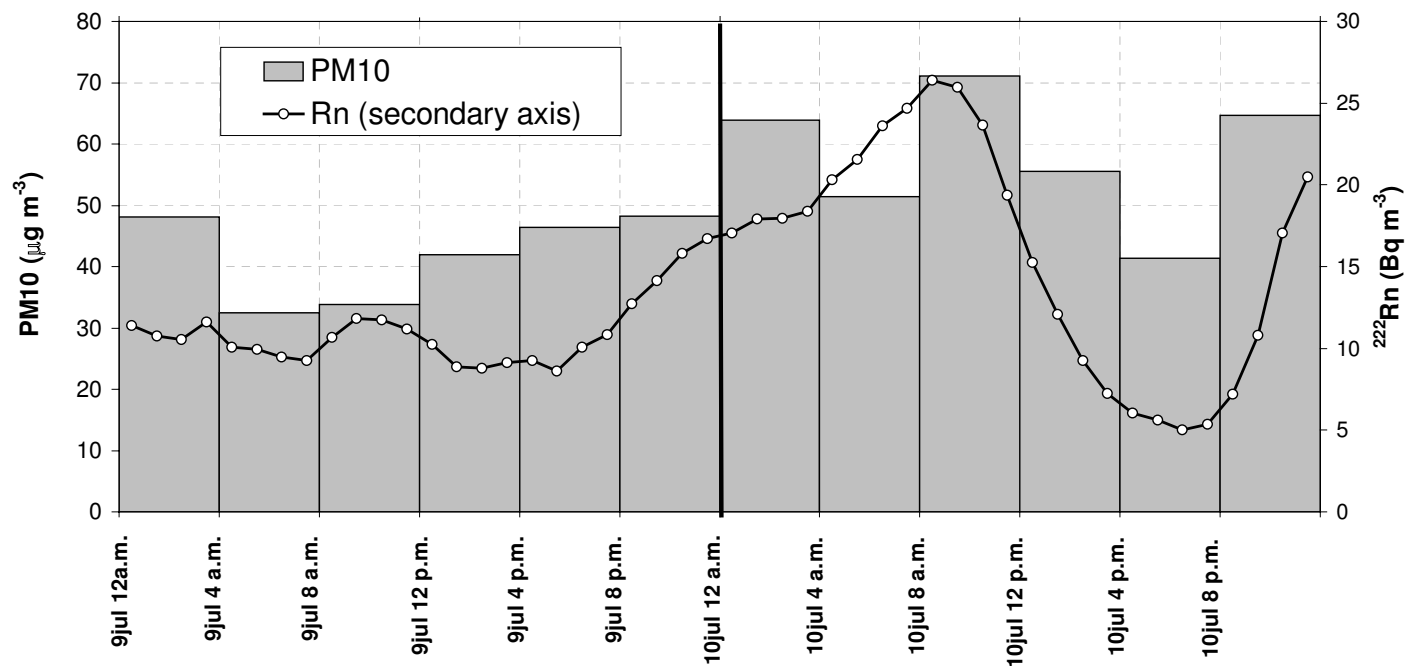
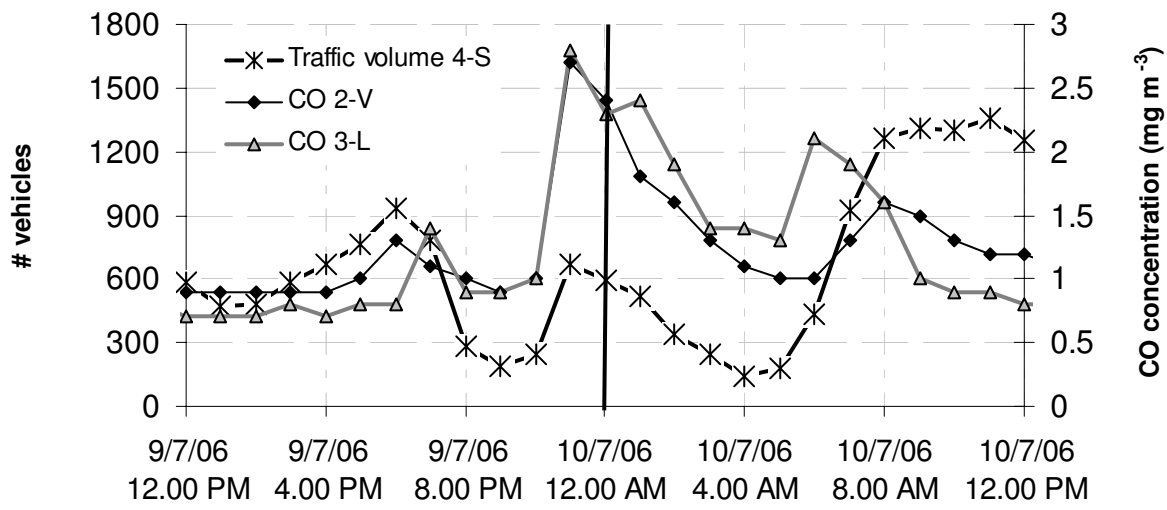
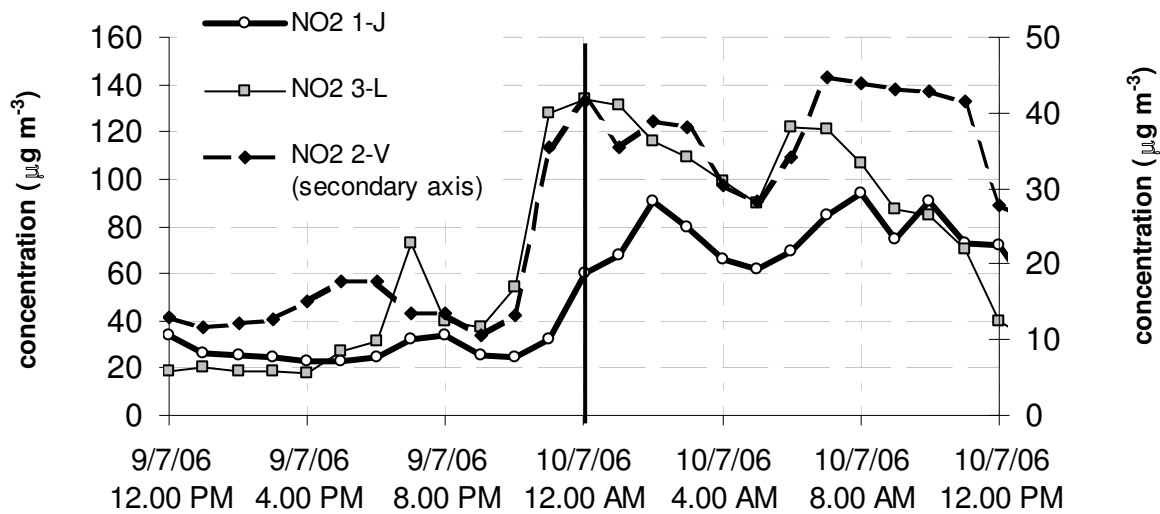


Figure 3



a)



b)

Figure 4

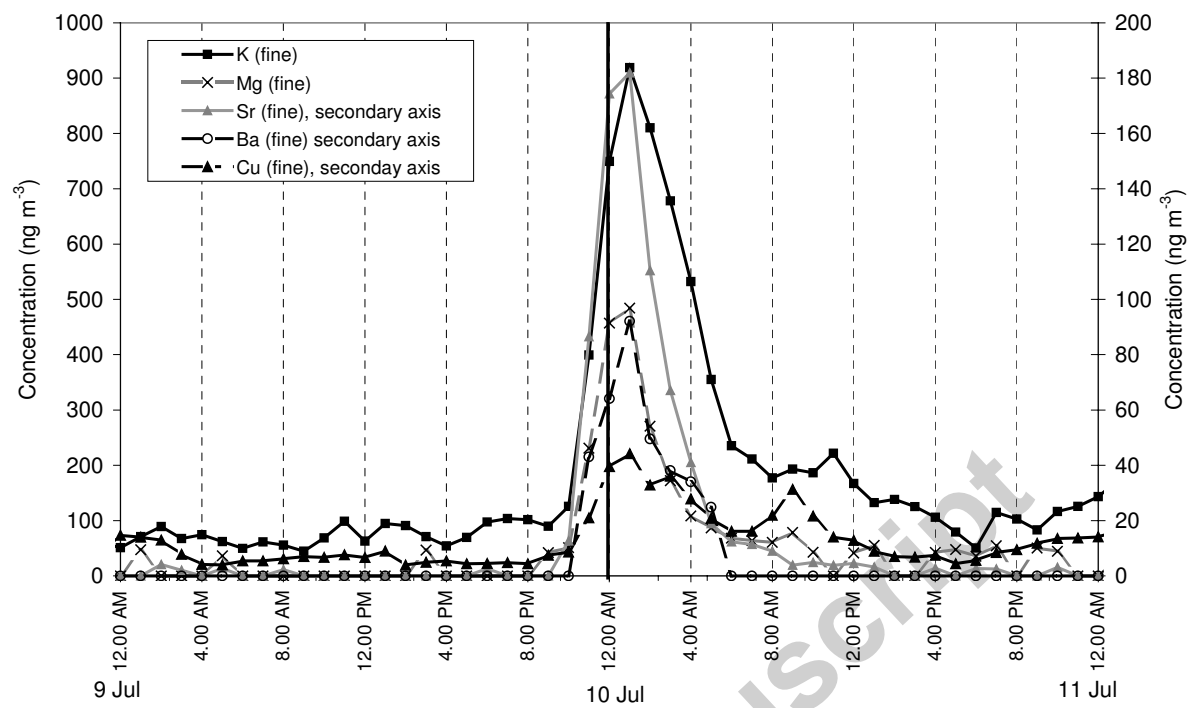


Figure 5

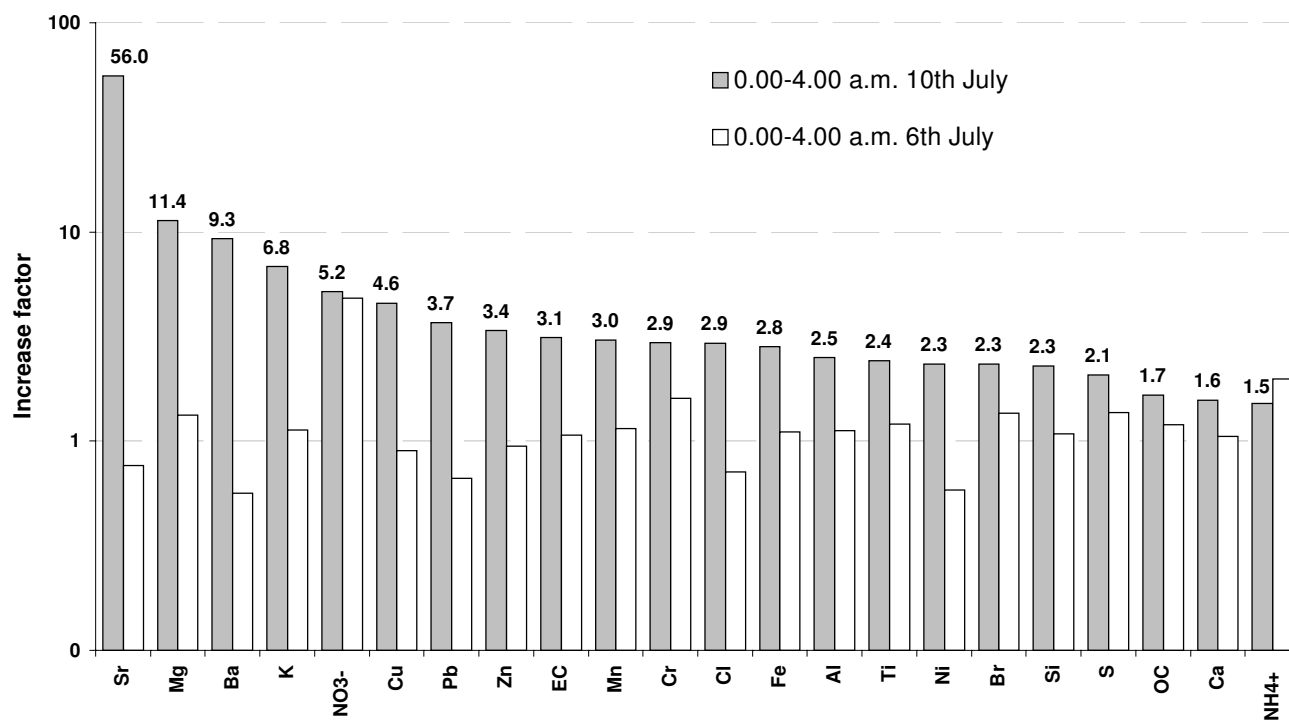


Figure 6

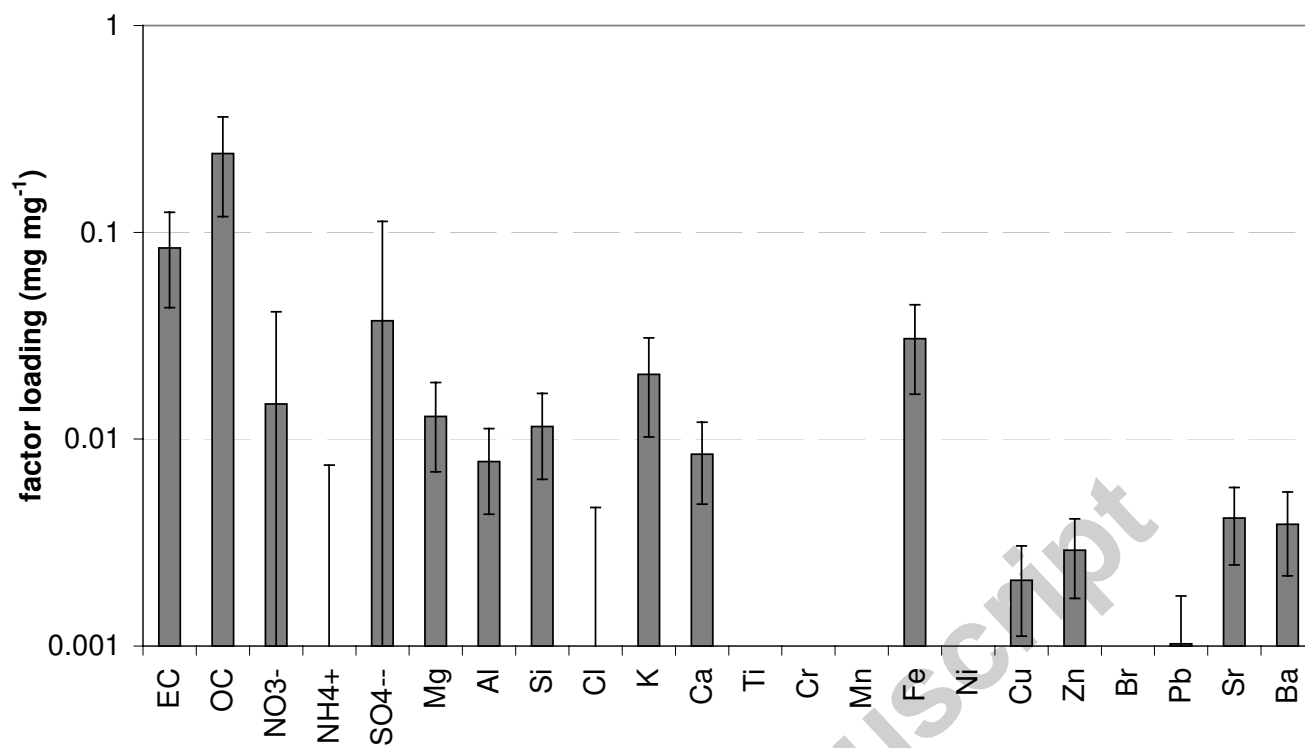


Figure 7

